RSC Advances

PAPER

View Article Online
View Journal | View Issue

Cite this: *RSC Adv.*, 2014, **4**, 7601

Effects of access resistance on the resistive-pulse caused by translocating of a nanoparticle through a nanopore†

Junrong Wang,[a] Jian Ma,[b] Zhonghua Ni,[b] Li Zhang[c] and Guoqing Hu*[a]

Received 22nd October 2013
Accepted 7th January 2014

DOI: 10.1039/c3ra46032k

www.rsc.org/advances

Recent experimental studies showed that the access resistance (AR) of a nanopore with a low thickness-to-diameter aspect ratio plays an important role in particle translocation. The existing theories usually only consider the AR without the presence of particles in the pore systems. Based on the continuum model, we systematically investigate the current change caused by nanoparticle translocation in different nanopore configurations. From numerical results, an analytical model is proposed to estimate the influence of the AR on the resistive-pulse amplitude, *i.e.*, the ratio of the AR to the pore resistance. The current change is first predicted by our model for nanoparticles and nanopores with a wide range of sizes at the neutral surface charge. Subsequently, the effect of surface charges is studied. The results show that resistive-pulse amplitude decreases with the increasing surface charge of the nanoparticle or the nanopore. We also find that the shape of the position-dependent resistive-pulse might be distorted significantly at low bulk concentration due to concentration polarization. This study provides a deep insight into the AR in particle-pore systems and could be useful in designing nanopore-based detection devices.

Introduction

The electrokinetically-driven translocation of a nanoparticle through a nanopore can be detected using Coulter's resistive pulse method. The Coulter counter was invented in 1953 by W. H. Coulter.[1] A typical Coulter counter consists of an insulating membrane containing a pore that separates two chambers containing electrolyte solutions. As a particle suspended in the solution traverses through the pore, it produces a change in the electrical resistance of the pore and therefore results in a current pulse. The height, width, and frequency of the pluses are related to the size, mobility, and concentration of the particles, respectively. The counters have been used widely in the analysis of microscale objects such as blood cells since the early years.[2–6] With the advances in microfabrication techniques in the last few decades, it is possible to produce nanoscale pores to analyze small biological particles such as DNA, RNA, proteins and virus.[7–11] The emerging need for the analysis of these nanoscale objects brings resurgence of interest in Coulter counting during the last 10 years.[12–15]

It is crucial to quantify the relation between the particle size and the resultant resistance pulse amplitude. Previous theoretical studies[16–20] have focused on solving the increase in resistance of a cylindrical pore caused by an insulating sphere far from the pore ends. These classic theories work well for the change of resistance inside the pore. Besides the pore's geometric resistance, the resistance of the medium outside the pore is called as access resistance (AR), which can be considered as the convergence resistance to a small circular pore from two semi-infinite reservoirs. In 1975, Hall[21] proposed a classic expression for the AR of an open pore as $R_a = 1/\kappa D$, where κ is the conductivity of the electrolyte and D is the diameter of the pore. In order to evaluate the effect of the AR, a parameter α can be introduced as the ratio of the AR to the pore's geometric resistance[22]

$$\alpha = R_a/R_p \quad (1)$$

At the open state, the resistance inside a cylindrical nanopore is $R_p = 4L/\pi\kappa D^2$, where L is the length of the nanopore. Then the influence of the AR at open state can be expressed as $\alpha = \pi D/4L$. Hence, the effect of the AR is significant for low thickness-to-diameter aspect ratios, which have their lengths being comparable to or even smaller than their diameter.

Early studies[23–27] on AR were mainly about the nanopores embedded in biological membranes, where the AR contributes

[a]*Institute of Mechanics, Chinese Academy of Sciences, Beijing 100190, China. E-mail: guoqing.hu@imech.ac.cn*

[b]*Jiangsu Key Laboratory for Design and Manufacture of Micro-Nano Biomedical Instruments, Southeast University, Nanjing 211189, China*

[c]*Research and Development Center, Synfuels China Technology Co., Ltd., Beijing 101407, China*

† Electronic supplementary information (ESI) available: A more detailed description of the mathematical model and the results of other nanopores. See DOI: 10.1039/c3ra46032k

10–30% to the total resistance. In the recent years, the AR of solid-state nanopores[28–32] has also been highly concerned. Compared with biological nanopores, the artificial nanopores drilled in solid membranes provide the ability to fabricate a wide range size of the nanopore with subnanometre precision. Although nanopores with thick membranes are still useful, modern fabrication techniques make it possible to achieve smaller pore lengths and lower aspect ratios, for example, solid-state nanopores in sub-10 nm silicon nitride membranes[8] and ultrathin single-layer graphene.[7,33,34] Such nanopores usually have higher spatial resolution to better analyze nanoscale objects.

Recently, several experiments on spherical nanoparticles trans-locating through lower aspect ratio nanopores have been carried out to investigate the relevant transport mechanisms.[22,35–38] Bacri *et al.*[36] studied the dynamics of colloids in single solid-state nanopore; however, they only considered resistance change inside the pore and found an overestimate current change. Tsutsui *et al.*[37] mimicked graphene nanopores by using an ultralow aspect ratio pore structure. They found that a constant AR assumption fitted their experimental measurements well. Under the hypothesis of invariant AR and α, Davenport *et al.*[22] systematically investigated the role of nanopore geometry in nanoparticle experiments using different aspect ratio nanopores. However, constant AR might not be able to predict the current change correctly in some cases, especially when particle's diameter is larger than pore's length.

Furthermore, at low bulk concentrations, the large surface area to volume ratio makes surface conductance play a key role in nanofluidic systems. Aguilella-Arzo *et al.*[26] numerically studied the AR and found that the AR of a nanopore in charged membranes was much lower than Hall's prediction. Recently, Lee *et al.*[39] experimentally and theoretically investigated the access effect of the conductance of different nanopores. However, those studies only considered ionic conductance of the open pores without the translocating particle.

In this work, a continuum model was developed to comprehensively study the effects of AR on the resistive-pulse caused by translocation of a particle through a nanopore. The model is verified by comparing the experimental results and classic theories. The influences of several important parameters, including particle size, pore aspect ratio, surface charge, and bulk concentration, on the change of AR were investigated. We also proposed analytical formulas that are able to effectively predict the resistive-pulse in various nanoparticle/nanopore systems.

Mathematical model

Fig. 1 shows the axisymmetric nanopore Coulter counter system for the particle detection. The nanopore has a circular cross sectional area of diameter D and length L, connecting two identical cylindrical fluid reservoirs. The lengths L_R and radius H_R of the reservoirs are large enough to be considered as infinite space. A nanopore system with higher D/L has larger reservoirs correspondingly in our computation. A typical reservoir size in our computation of the $D = 5L = 250$ nm nanopore system is

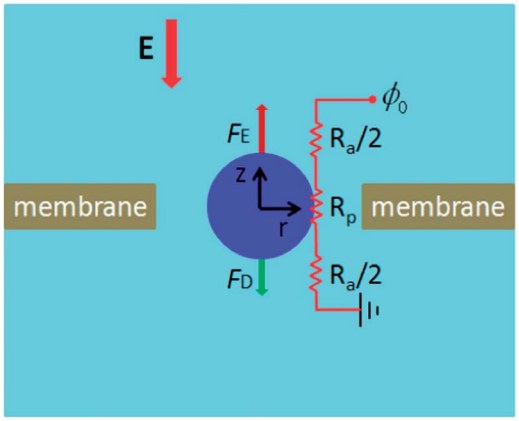

Fig. 1 A schematic depiction of the nanopore system used in this study. The charged particle translocates through the nanopore under applied electric field, experiencing an electrophoretic force F_E and a hydrodynamic drag F_D stemming from electroosmosis.

$L_R = 5$ μm and $H_R = 10$ μm. The nanopore and the reservoirs are filled with an electrolyte solution. A spherical nanoparticle of diameter d moves along the axis of the nanopore. An applied voltage across the two electrodes embedded at the reservoir ends is used to attain ionic current and drive the nanoparticle translocating through the nanopore.

The Laplace model

Since bulk conductance is directly proportional to the bulk concentration, surface conductance stemmed from surface charge can be generally neglected at high bulk concentrations for nanopore systems. When there is no or negligible surface charge on the particle and the nanopore walls, the electrolyte solution is neutral everywhere. In this circumstance, the distribution of electrical potential ϕ can be obtained by solving the Laplace's equation, which is derived from Gauss's law for neutral solution

$$\nabla^2\phi = 0 \tag{2}$$

and the electrical current density $\boldsymbol{J}$ is given by

$$\boldsymbol{J} = -\kappa\nabla\phi \tag{3}$$

where κ is the conductivity of the electrolyte solution. A specified potential, ϕ_0, was applied at the reservoir ends, and a electric insulation condition was set on all walls, $\mathbf{n}\cdot\nabla\phi = 0$, where $\mathbf{n}$ is the unit outer normal vector.

The ionic current through the nanopore is integrated as $I = \iint_{A(z)} \boldsymbol{J}\cdot\mathbf{n}\mathrm{d}A(z) = -\iint_{A(z)} \kappa\frac{\partial\phi}{\partial z}\mathrm{d}A(z)$, where $A(z)$ is the cross sectional area perpendicular to the length coordinate z.

The PNP–NS model

When the surface charge of particle or nanopore cannot be neglected, especially for nanopore system at low bulk concentrations, there is non-neutral region of the ionic solution near charged surfaces due to the requirement of overall

electroneutrality, resulting in a failure for the Laplace model to simulate ionic current. Based on the continuum approximation at the nanoscale,[40] the governing equations in this circumstance are the Poisson–Nernst–Planck (PNP) equations for the electrostatic potential distribution and the ionic mass transport and the Navier–Stokes equations (NS) for the liquid flow, as follows:[41–46]

$$\nabla^2\phi = -\frac{\rho_e}{\varepsilon_0\varepsilon_r} \quad (4)$$

$$\frac{\partial c_i}{\partial t} + \nabla\cdot J_i = \frac{\partial c_i}{\partial t} + \nabla\cdot\left(- D_i\nabla c_i + \mathbf{u}c_i - \frac{z_iFD_i}{RT}c_i\nabla\phi\right) = 0 \quad (5)$$

$$\nabla\cdot\mathbf{u} = 0 \quad (6)$$

$$\rho\left(\frac{\partial\mathbf{u}}{\partial t} + \mathbf{u}\cdot\nabla\mathbf{u}\right) = \mu\nabla^2\mathbf{u} - \nabla p - \rho_e\nabla\phi \quad (7)$$

where p is pressure, $\mathbf{u}$ is the velocity vector,ε_0 is the electrical permittivity of vacuum, ε_r is the relative permittivity of solution, ρ is the fluid density, μ is the fluid viscosity, F is the Faraday's constant, R is the molar gas constant, T is the temperature, and z_iFD_i/RT is the electrophoretic mobility obtained from the Nernst–Einstein relation; J_i, D_i, c_i, and z_i are the flux, the diffusivity, the concentration, and the valence of the each ionic species, respectively. Here ρ_e is the net charge density of the ionic species, which is given by $\rho_e = F\sum_{i=1}^{n} z_ic_i$, where n is the number of ionic species involved in the system.

Boundary conditions are also provided for closure of the PNP–NS equations. To solve the Poisson's equation (eqn (4)), a specified potential, ϕ_0, was applied at the ends of the two reservoirs, and the specified surface charge densities were set on the particle surfaces, $-\mathbf{n}\cdot\nabla\phi = \sigma_p/\varepsilon_0\varepsilon_r$, and the nanopore surfaces, $-\mathbf{n}\cdot\nabla\phi = \sigma_n/\varepsilon_0\varepsilon_r$. To solve the Nernst–Plank equations (eqn (5)), the ionic concentrations were maintained at their bulk values on the ends of the two reservoirs, $c_i = c_{bulk}$, and ion-impenetrable conditions were assumed on all other boundaries, yielding $\mathbf{n}\cdot J_i = \mathbf{n}\cdot(\mathbf{u}c_i)$.[42] To solve the fluid flow field (eqn (6) and (7)), a normal flow with zero pressure was applied on the ends of the two reservoirs, and non-slip boundary conditions were assumed on all other solid walls, yielding $\mathbf{u} = \mathbf{u}_p$ on the particle surfaces and $\mathbf{u} = 0$ on other walls. The translocation velocity of the particle, $\mathbf{u}_p$, can be found by satisfying the force balance on the particle.[42,47]

Under a quasi-steady approximation,[47,48] which assumes that all the physical fields reach quasi-steady state at any moment, we can neglect the unsteady terms from the Nernst–Planck equation and Navier–Stokes equation in our nanopore system.

Finally, the ionic current through the nanopore is also integrated as

$$I = \iint_{A(z)} F\left(\sum_{i=1}^{N} z_iJ_i\right)\cdot\mathbf{n}\mathrm{d}A(z) \quad (8)$$

Note that the ionic flux consists of diffusion, convection, and electromigration in the Nernst–Plank equations (eqn (5)). When there is no or negligible surface charge on the particle and the nanopore walls, the ionic solution is neutral and the concentration of the each ionic species is the bulk value everywhere. Therefore, the convection and the diffusion do not cause a change in the electrical current and the current solely comes from the ionic migration in electric field. As a result, eqn (8) can be simplified to eqn (3) for uncharged case, where the conductivity of the solution in eqn (3) is expressed as $\kappa = \sum_{i=1}^{N} z_i^2F^2D_ic_{bulk}/RT$.[49]

A more detailed description of the mathematical model is presented in the ESI.†

Resistance analysis

In our study, the nanopore system behaves as a linear Ohmic resistor. The most useful approximation for the pore's geometric resistance is

$$R_p = \frac{1}{\kappa}\int_{-L/2}^{L/2}\frac{\mathrm{d}z}{A(z)} \quad (9)$$

However, this equation implies that the current density is uniform across each cross section, and any deviations from uniformity will give a larger resistance.[17] For the large particle limit (*e.g.*, $d/D \geq 0.9$), where the cross section of the blocked pore changes slowly with length, the resistance change inside the pore can be obtained by extending eqn (9):[16,36]

$$\frac{\Delta R_p}{R_p} = \begin{cases} \dfrac{D}{L}\left[\dfrac{\arcsin(d/D)}{\left(1-(d/D)^2\right)^{1/2}} - \dfrac{d}{D}\right], & d \leq L \\ \dfrac{D}{L}\left[\dfrac{\arctan\left(L/D\Big/\left(1-(d/D)^2\right)^{1/2}\right)}{\left(1-(d/D)^2\right)^{1/2}} - \dfrac{L}{D}\right], & d > L \end{cases} \quad (10)$$

In 1977, Deblois *et al.*[18] proposed a simple empirical form

$$\frac{\Delta R_p}{R_p} = \frac{d^3}{D^2L}\frac{1}{1-0.8(d/D)^3} \quad (11)$$

which is believed accurate for calculating the resistance changes for intermediate particles limit ($d/D = 0.2$–0.9) in long pores.

In the present study, we define the current change as $\Delta I/I = (I_o - I_b)/I_o$, where the subscript 'o' or 'b' represents open state or blocked state, respectively. The relation between the current change and the resistance change is

$$\frac{\Delta I}{I} = \frac{1/(R_{op}+R_{oa}) - 1/(R_{bp}+R_{ba})}{1/(R_{op}+R_{oa})} \quad (12)$$

where the second subscript on resistance with an 'a' or 'p' represents AR or pore resistance, respectively. The pore resistance change can be obtained by classic theory. Although Hall gave a classic equation for AR at the open state, no analytic expression exists for the AR at the blocked state. In this work, we try to develop a correlation equation to estimate the blocked AR in accordance with our numerical results.

Results and discussion

In this section, we present our numerical results of the nanopore systems with various ratios of L/D or d/D. We assume a constant nanopore length $L = 50$ nm, and a wide range D/L from 0.1 to 10.

We focus on the effects of the AR on the resistive-pulse amplitude caused by nanoparticle translocating along the axis of the nanopore. We studied two cases: (i) neutral or negligible surface charges at high bulk concentrations and (ii) significant surface charges at low bulk concentrations.

Model validation

The numerical simulations are performed with the finite element software package COMSOL 4.0 (Comsol, Inc.). Grid checks are performed to ensure the grid independence of the numerical solution.

In order to verify our models, the numerical results were first compared with classic analytical results for a long channel without reservoirs. Fig. 2 shows a comparison of resistive-pulse amplitude ($\Delta I/I$) caused by a spherical particle with relative particle size (d/D) ranging from 0.2 to 0.9. The Laplace model is used for neutral situations, and the PNP–NS model deals with a particle immersed in 100 mM KCl with -10 mC m^{-2} on the particle and nanopore walls. Good agreement is found between our two models. In addition, our numerical results agree very well with the classic theory of the intermediate particles limit.

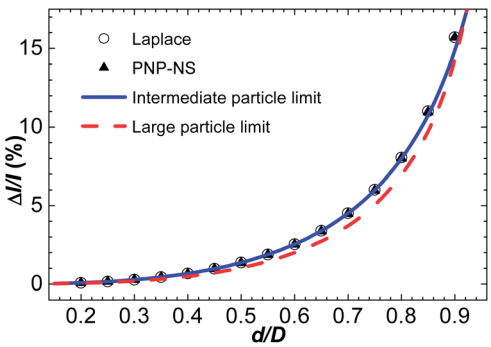

Fig. 2 Comparisons of our two models and two classic theoretical predictions on resistive-pulse amplitude caused by a spherical particle with wide sizes in a long channel ($L/D = 10$) without reservoirs. Here, the intermediate particles limit is eqn (11) and the large particles limit is eqn (10).

We then compared our numerical results with the experimental data of Bacri *et al.*[36] and Davenport *et al.*,[22] as shown in Table 1. This table also lists the results of two other analytical models: (i) the model without AR, which only considers the resistance change inside the pore, is used in the work of Bacri *et al.*,[36] and (ii) the model with constant AR, which is the results of the no AR model divided by $(1 + \alpha_o)$, is similar to the approximate formula used in the work of Davenport *et al.*[22] Our numerical results give more accurate values than the model without AR. In some cases, the model with constant AR can also produce satisfactory results compared to the experimental measurement.

The particle and the nanopore surfaces are uncharged

The detection of nanoparticles with nanopores is usually performed at high bulk concentrations (*e.g.*, 100 mM or higher),[7–9,22,33,34] where the Laplace model with no surface charges and the PNP–NS model with typical surface charges give almost identical results. Therefore, we used Laplace model to simulate the cases at high salt concentrations.

We first consider a nanopore system with $D = L$. Generally, the resistive-pulse height achieves its maximum value when the particle's center coincides with the axial center of the nanopore. Since the particle diameter d must be smaller than the nanopore diameter D, the whole particle will be located completely inside the nanopore when the resistive-pulse magnitude reaches its maximum value. Fig. 3(a) show the current streamline passing a particle with $d/D = 0.5$ in the nanopore system with $D = L = 50$ nm. The current streamline outside the pore is slightly affected by the blocked particle, resulting in a slight change of the AR. By comparing the computed resistances at the open state and the blocked state, we found that the change in the AR is about 2% of the change in the pore resistance. Thus it is reasonable to assume an invariant AR on estimating the resistive-pulse amplitude, and eqn (12) becomes

Table 1 Comparisons of the resistive-pulse amplitude between experimental results, the present simulation and two other analytical models. We used the Laplace model for the present simulation. The model without AR neglects the AR in eqn (12) and the model with constant AR uses the hypothesis of invariant AR and α during particle translocation. Aqueous electrolyte solution was 10 mM KCl in the work of Bacri *et al.*, and 100 mM KCl in the work of Davenport *et al.*

			$\Delta I/I$			
References	Nanopore size[a] (nm)	Particle size (nm)	Experiment results	The present simulation	Model without AR	Model with constant AR
Bacri *et al.*[36]	50 × 156[b]	85	13.0	10.9	26.4	7.65
Davenport *et al.*[22]	50 × 260	57	0.76	0.53	3.59	0.71
	50 × 260	101	2.57	3.00	13.8	2.73
	100 × 260	57	1.15	0.62	1.86	0.61
	100 × 260	101	4.95	3.48	10.4	3.40

[a] We use the form of $L \times D$ to express a nanopore size in this table. [b] The pore in the work of Bacri *et al.* has a oval cross section with diameter (140 × 175) nm, so we choose a equivalent circle with diameter 156 nm here.

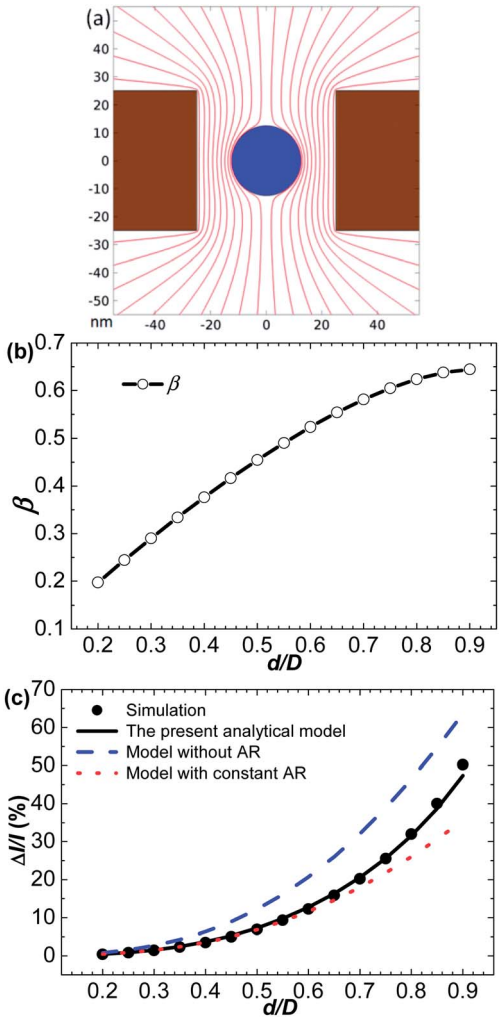

Fig. 3 Numerical results for the nanopore system with $D = L = 50$ nm. (a) The current streamline around a particle of $d/D = 0.5$ at the center. (b) The computed values of β. (c) Comparisons of the numerical results and different analytic models on resistive-pulse amplitude, and here the present analytical model is eqn (13) and (14) with $\beta = 0.5$.

$$\frac{\Delta I}{I} = \frac{R_{bp} - R_{op}}{R_{bp} + R_{ba}} = \frac{R_{bp} - R_{op}}{R_{bp}} \frac{1}{1 + \alpha_b} \tag{13}$$

where the part $(R_{bp} - R_{op})/R_{bp}$ can be obtained using the classic theory $(R_{bp} - R_{op})/R_{bp} = 1-1/(1 + \Delta R_p/R_p)$.Then we need the blocked value of α, which depends on the particle relative diameter d/D, to estimate the resistive-pulse amplitude.

Based on the numerical results, we propose an analytical expression for the blocked value of α:

$$\alpha_b = \alpha_o(1 - d^2/D^2)^\beta \approx \pi D(1 - d^2/D^2)^\beta/4L \tag{14}$$

where β is a correction factor. In our simulations, the calculated AR at the open state was slightly larger than Hall's result.

Fig. 3(b) shows the computed value of β varies from 0.2 to 0.65 with the relative particle diameter d/D ranging from 0.2–0.9. We did not find a simple analytical relationship between the value of β and the relative particle diameter. Fortunately, since the value of $(1 - d^2/D^2)$ is close to unit for small particle diameters, the corresponding value of α_b is thus approximate to the value of α_o and insensitive to the choice of β. Therefore, we can use a fixed value like $\beta = 0.5$ in eqn (14) to estimate α_b and then get the resistive-pulse amplitude by eqn (13).

The resistive-pulse amplitude predicted by eqn (13) and (14) with $\beta = 0.5$ agrees very well with the numerical simulations, as shown in Fig. 3(c). Compared to the numerical results, the model without AR has significant deviation while the model with constant AR gives good prediction of resistive-pulse amplitude only for $d/D \leq 0.5$. Actually, since the value of α_b is close to the corresponding value of α_o for small particles ($d/D \leq 0.5$), the model with constant AR can be considered as a simplified form of the present analytic model.

Next, we consider a lower aspect ratio nanopore system with $D = 5L$. If the relative particle diameter d/D is larger than 0.2, a part of the particle will be outside the nanopore, which directly affects the AR, as shown in Fig. 4(a).

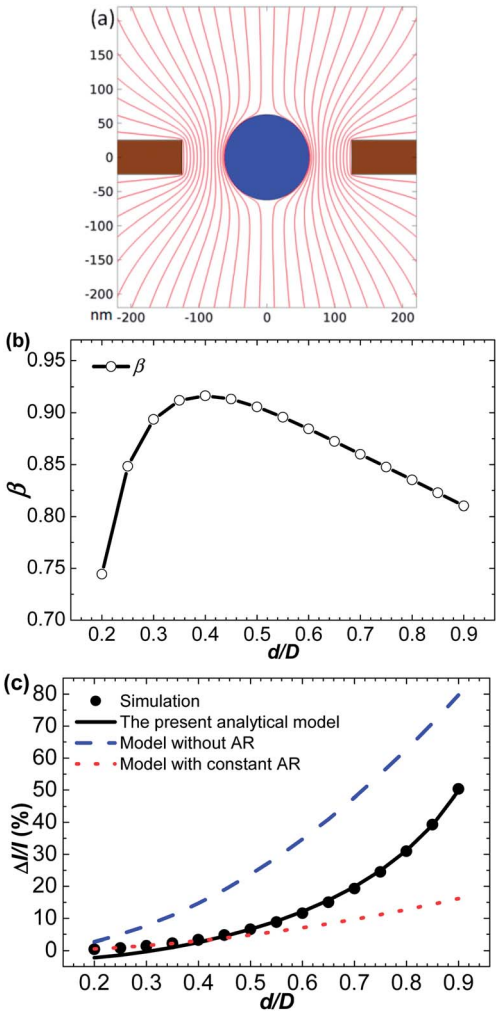

Fig. 4 Numerical results for the nanopore system with $D = 5L = 250$ nm. (a) The current streamline around a particle of $d/D = 0.5$ at the center. (b) The computed values of β. (c) Comparisons of the numerical results and different analytic models on resistive-pulse amplitude, and here the present analytical model is eqn (15) and (14) with $\beta = 0.8$.

From our numerical simulations, we found that the AR change between the open state and the blocked state is about −30–30% of the pore resistance change for the relative particle diameter d/D ranging from 0.2 to 0.9. To get more accurate analysis, it is inappropriate to assume constant AR any more. From eqn (12), we get

$$\frac{\Delta I}{I} = 1 - \frac{R_{op} + R_{oa}}{R_{bp} + R_{ba}} = 1 - \frac{(1 + \alpha_o)}{(1 + \alpha_b)} \frac{R_{op}}{R_{bp}} \quad (15)$$

where the part R_{op}/R_{bp} can be obtained by $R_{op}/R_{bp} = 1/(1 + \Delta R_p/R_p)$. Since the cross section of the ultralow aspect ratio pore blocked by a nanoparticle changes slowly with length, the large particle limit of the classic theory can be applied here.

Fig. 4(b) shows the value of correction factor β varies from 0.72 to 0.9 with the relative particle diameter d/D ranging from 0.2–0.9. The value of β is not monotonous with the change of relative particle diameter. Nevertheless, we still try to use a constant β to estimate α_b and the resistive-pulse. Using a fixed $\beta = 0.8$, we found that the relative errors of estimated α_b to the numerical results were within 3%.

We then used eqn (15) and (14) with $\beta = 0.8$ to predict the resistive-pulse amplitude. As shown in Fig. 4(c), our model provides better agreement with the numerical results than the previous models. Unfortunately, because of the mathematical nature of eqn (15), a small error in estimated α_b or pore resistance change will significantly affect the current change with small values (*e.g.*, $\Delta I/I \leq 5\%$). Since the AR change is within 30% of the pore resistance change, the model with constant AR has smaller errors to estimate the resistive-pulse amplitude for small particles ($d/D \leq 0.4$), as shown in Fig. 4(c).

We have also simulated various nanopore systems with D/L ranging from 0.1 to 10. It is convenient to normalize the Laplace model and obtain the same $\Delta I/I$ for a given particle-nanopore system with the same L/D and d/D ratios. More details of the dimensionless Laplace model and the results of other nanopores are presented in the ESI.†

For nanopore systems with $D < L$, the eqn (13) and (14) with $\beta = 0.5$ are also adequate to predicate the resistive-pulse amplitude. The effect of the AR decreases with decreasing D/L, for example, the relative error between the numerical results of the nanopore system with $D = 0.1L$ and the model without AR is within 10%. For nanopore systems with $D > L$, it was suitable to use eqn (15) and (14) with $\beta = 0.8$ to approximately get the resistive-pulse amplitude for particle with $d/D \geq 0.4$. The hypothesis of invariant AR may be also acceptable for small particles in nanopores with $D/L \leq 5$, while there might be considerable error of the current change in nanopore systems with larger D/L.

So far we have proposed analytical equations to estimate the effect of the AR in nanopore systems with nanoparticles. However, these expressions are still not concise enough to predict resistive-pulse amplitude. We then tried to develop a simple method to estimate the resistive-pulse amplitude.

Since the resistance change is a result of excluded electrolyte solution by the particle, some previous studies simply considered the pulse height as the third power of the particle diameter for high aspect ratio pores.[12,17] Following this line and assuming the cubic relation for low aspect ratio nanopores, we construct the following equation to estimate the resistive-pulse amplitude

$$\Delta I/I = 8(d/D)^3 \cdot (\Delta I/I)_{d/D=0.5} \quad (16)$$

where the $(\Delta I/I)_{d/D=0.5}$ is the current change of $d/D = 0.5$, and is used here as a reference value. We define the relative error of $\Delta I/I$ estimated by eqn (16) to that of our numerical results as RE $-\Delta I/I$.

Fig. 5(a) shows the values of RE $-\Delta I/I$ for the nanopore systems with $D = L$ and $D = 5L$. We can see that the relative error is within 10% for $d/D \leq 0.7$. For larger particles, it may be more suitable to use our previously proposed equations. We also calculated other nanopore systems with D/L ranging from 0.1 to 10, and got similar results. The relative errors were smaller than 10% for $d/D \leq 0.7$, even for ultralow aspect ratio pores. It indicates that the hypothesis of cube relation on the current change is acceptable for small particles ($d/D \leq 0.7$) in wide aspect ratio range, even when the particle diameter is larger than the nanopore length. We calculated the current change for $d/D = 0.5$ with D/L ranging from 0.1 to 10, as shown in Fig. 5(b). Interestingly, there is a maximum value of the current change for $D/L \sim 2$, which suggests that a nanopore with optimized aspect ratio may increase the detection sensitivity.

We can also extend our analytical model for cylindrical particles (*e.g.*, DNA). For ultralow aspect ratio nanopores, a large

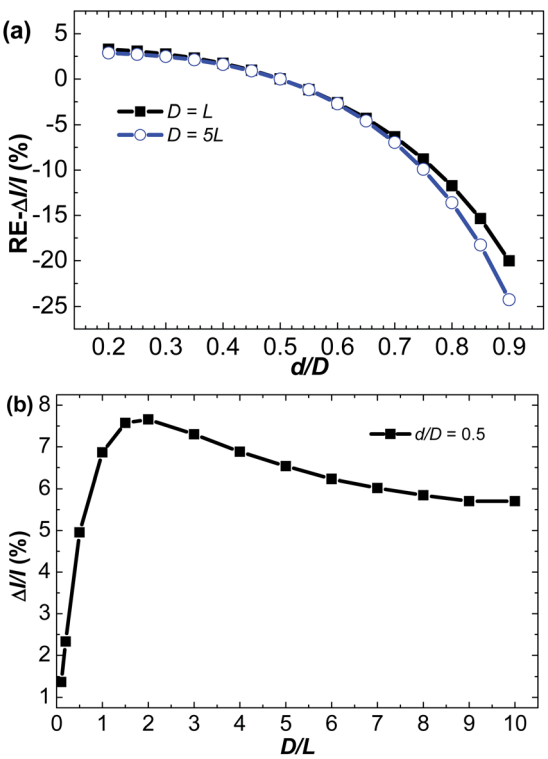

Fig. 5 (a) The relative errors of the resistive-pulse amplitude estimated by eqn (16) to that of our numerical results for the nanopore systems with $D = L$ and $D = 5L$. (b) Numerical results for resistive-pulse amplitude caused by particles with $d/D = 0.5$ in nanopore systems with D/L ranging from 0.1 to 10.

spherical particle is approximate cylindrical inside the pore, but causes less change on the AR than a cylindrical particle with the same diameter. Thus, we consider a cylindrical particle as a limit case for large particles. The numerical results demonstrated that the values of β are about 0.77 for d/D ranging from 0.2 to 0.9 in a nanopore system with $D = 5L$, as shown in Fig. 6(a). Fig. 6(b) shows that eqn (15) and (14) with $\beta = 0.77$ provide excellent agreement with our numerical results on resistive-pulse amplitude for cylindrical particles with a wide size. We also calculated various nanopore systems with D/L ranging from 0.1 to 10, and found a constant $\beta = 0.77$ was acceptable in all nanopore systems.

The particle and the nanopore surfaces are charged

Sometimes nanoparticles are driven through nanopores at low bulk concentrations (*e.g.*, 10 mM or lower),[10,36,37] where the surface charges on the particle and the nanopore have significant effects on regulating the ionic current. The PNP–NS model is needed to treat the transport phenomena when the surface charges exist. Without loss of generality, we chose negative surface charge for both particle and nanopore to prevent the nanoparticle from being electrostatically absorbed by the nanopore walls.

The open state was considered first. Due to excess counterions stemming from the surface charges, the pore resistance decreases once the nanopore surfaces are charged. Taking account of the effect of surface charges as the surface conductance, we get the resistance inside the nanopore with charged walls as

$$R_{op} = \left[\kappa_b \frac{\pi D^2}{4L} + \kappa_s \frac{\pi D}{L}\right]^{-1} \quad (17)$$

where κ_b is the bulk conductivity and κ_s is the surface conductivity. At low salt concentrations, the conductivity of the solution scales with the ionic concentration and $\kappa_s/\kappa_b \approx |\sigma_n|/(2Fc_{bulk})$.[39]

If the nanopore walls are charged, the open pore resistance decreases as a result of the counterion accumulation near the pore entrance due to the surface charge. Recently, Lee *et al.*[39] proposed an approximate equation for AR, which can be rewritten as

$$R_{oa} = [2\kappa_b D + \gamma\kappa_s]^{-1} \quad (18)$$

where γ is a numerical constant. While $\gamma = 2$ was used in Lee's work, we found that $\gamma = 3$ is the best match for our numerical results. From eqn (17) and (18), we can get an analytic expression for α_o as the ratio of the AR to the pore resistance at the open state.

$$\alpha_o \approx \frac{Fc_{bulk}\pi D^2 + 2\pi D|\sigma_n|}{8Fc_{bulk}DL + 6|\sigma_n|L} \quad (19)$$

Fig. 7(a) and (b) shows that the α_o increases as the surface charge density of the nanopore surfaces increase in 10 mM KCl

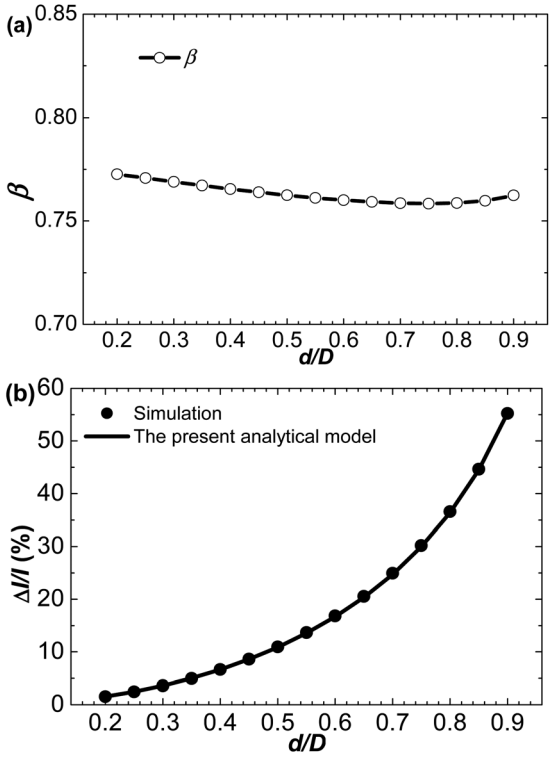

Fig. 6 Numerical results for a long cylindrical particle with different sizes in the nanopore system with $D = 5L$. (a) The computed values of β. (b) Comparison of the numerical results and the present analytic model with eqn (15) and (14) with $\beta = 0.77$ on resistive-pulse amplitude.

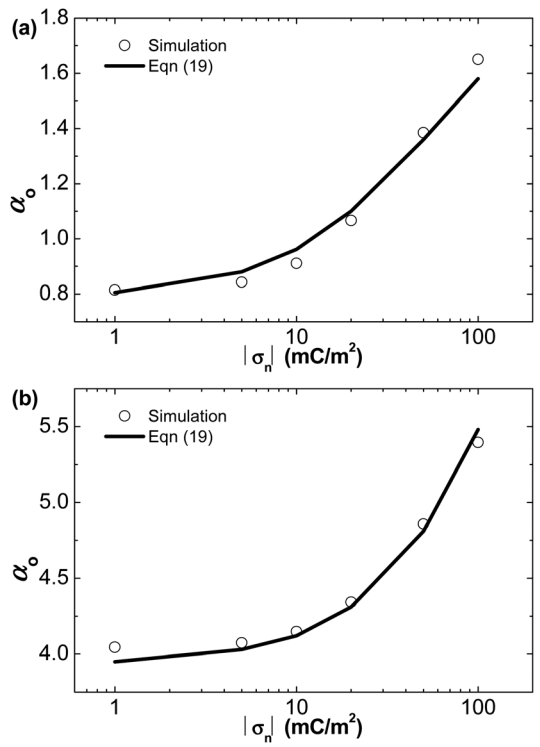

Fig. 7 Comparison of the open α_o obtained from numerical simulation and predicted by eqn (19) as a function of the nanopore surface charge density in a nanopore system with (a) $D = L = 50$ nm and (b) $D = 5L = 250$ nm. The bulk electrolyte solutions are 10 mM KCl.

solution. Two typical nanopore configurations with $D = L =$ 50 nm and $D = 5L = 250$ nm were investigated here. It is found that the eqn (19) for α_o fits our numerical results well. Although the pore resistance and the AR both decrease as the nanopore walls are charged more, the change of the pore resistance is larger than that of the AR, leading to an increased α_o.

Next, we consider the blocked state. We assume a typical surface charge density, -10 mC m^{-2}, on both the particle and nanopore surfaces with10 mM bulk concentration. Fig. 8(a) and (b) depict the comparison of computed values of α_b in charged and neutral cases with the relative particle diameter d/D ranging from 0.2–0.9. The blocked values of α_b for a wide size particle become larger in charged case. The difference between values for α_b slightly increases for larger particles. It is hard to get an analytical expression for blocked α_b in charged case. To get the accurate analysis, numerical simulations with the PNP–NS model should be applied.

Because of limitations in space, we only consider particles with $d/D = 0.5$ for the current change. Using a fixed surface charge density, -10 mC m^{-2}, on the nanopore surface or the particle surface, we changed the charge densities from -1 to -100 mC m^{-2} on the particle surface or the nanopore surface, respectively. Under a 10 mM bulk concentration, as the surface charge density on the particle surface increases, more counterions accumulate near the particle surface to compensate the excluded ions. Therefore the current change caused by the particle decreases, as shown in Fig. 9(a). When the nanopore surfaces are charged more, more counterions accumulate inside the nanopore, leading to decrease the resistance change inside the pore. From our numerical results, the current change in both nanopore systems also decreases as the nanopore surfaces are charged more, as shown in Fig. 9(b). When the nanopore surface charge density is about -100 mC m,$^{-2}$ the current change may decrease to half or even lower.

Since the surface conductance is more significant at lower bulk concentration, it is necessary to study the effects of the bulk concentrations. We assume identical surface charge density, -10 mC m^{-2}, on both the particle and the nanopore surfaces. As the bulk concentration of solution decreases, the current change decreases, as shown in Fig. 9(c). At low enough bulk concentrations, the blocked current may be larger than the open current in the $D = L$ nanopore system with

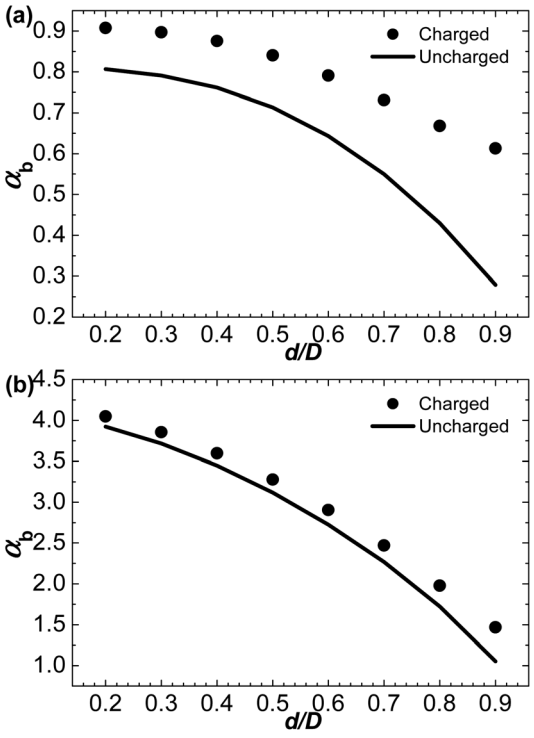

Fig. 8 Comparison of the blocked α_b between charged and uncharged cases in a nanopore system with (a) $D = L = 50$ nm and (b) $D = 5L = 250$ nm. The surface charge densities on both the particle and nanopore walls are assumed to be -10 mC m^{-2} for charged cases. The bulk electrolyte solutions are 10 mM KCl.

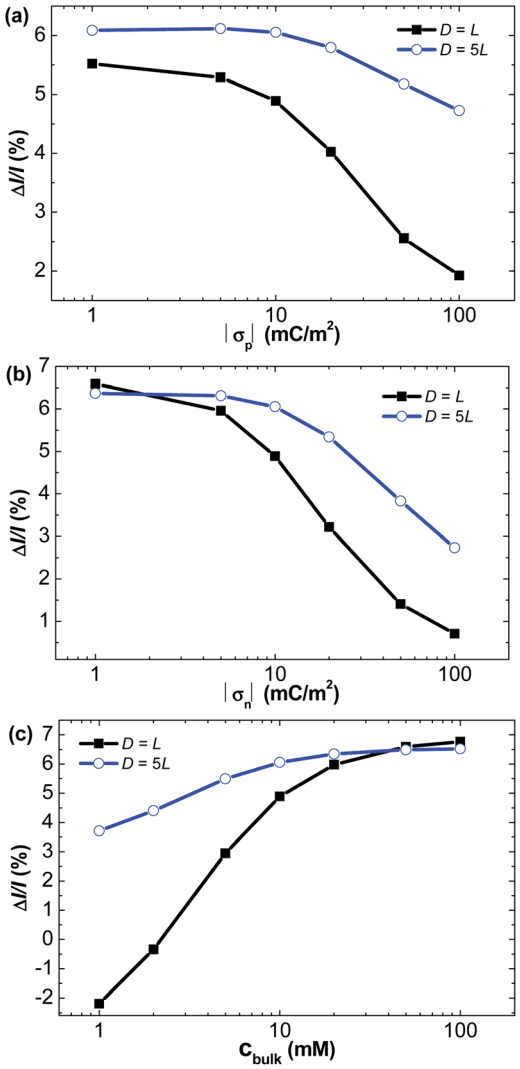

Fig. 9 Numerical results of the current change caused by a particle ($d/D = 0.5$) for the $D = L$ and $D = 5L$ nanopore systems as a function of (a) the surface charge density of the nanopore surface, (b) the surface charge density of the nanoparticle surface, and (c) different bulk concentrations. The bulk concentration in (a) and (b) is 10 mM. The surface charge densities on both the particle and nanopore walls in (c) are -10 mC m^{-2}.

$d/D = 0.5$. This indicates that the resistance pulse may be reversed, for example, DNA translocation in low bulk concentrations,[50] where the excess counterion stemmed from DNA molecule surface charge may be larger than the excluded ions.

Transitional current change caused by particle translocation

Finally, we consider the particle at different axial positions of the nanopore system. Fig. 10(a) depicts the current changes caused by a particle ($d/D = 0.5$) translocating through the $D = 5L = 250$ nm nanopore system along z axis. We assume -10 mC m^{-2} on both the particle and nanopore surfaces with different bulk concentrations ranging from 1 mM to 100 mM.

At high bulk concentration, we got a position-dependent bell-shaped current change. Similar to previous simulation works,[17,32] the ionic current starts to change when the particle is approximately one pore diameter away from the pore mouth. Such current change could be used to determine the corresponding position of resistive pulse width in experiments.[19] However, it is hard to determine the exact start position for experiments with considerable current noise. From our numerical results of 100 mM, the current change is only about 1% of its maximal value when the particle is one pore diameter away from the pore mouth, and the corresponding position of a 10% of the maximum relative current change is about half pore diameter away from the pore mouth. The latter position may be also useful in experiments to estimate particle translocation velocity.

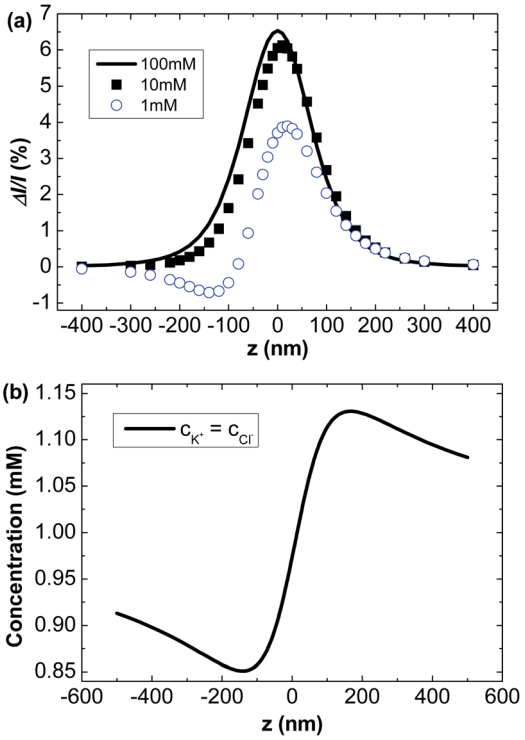

Fig. 10 (a) Numerical results of the current change caused by a particle ($d/D = 0.5$) translocating through the $D = 5L = 250$ nm nanopore system along z-axis with the bulk concentrations ranging from 1 mM to 100 mM. (b) The ionic concentration distribution on the z-axis at 1 mM bulk concentration for the open state.

The resistance pulse is symmetric at high bulk concentration. However, we noted that the particle position of the maximum current change is slightly biased from the middle-point of the nanopore at low bulk concentrations. Moreover, the blocked current may be larger than the open current at 1 mM at some positions. We attribute these unique phenomena to ionic concentration polarization (CP) caused by external electric field.[51] Fig. 10(b) demonstrates that the ionic concentration is slightly smaller than the bulk value at the anode side near the nanopore mouth and *vice versa* at the other side. Since the nanopore diameter is much larger than the thickness of the electrical double layer (EDL), which is a shielding layer near a charged surface and is about 10 nm at 1 mM bulk concentration, the concentrations of K^+ and Cl^- are identical along the z-axis in the central part of the nanopore. A blocked particle mainly affects the bulk conductance. When the particle reaches the low concentration region, it causes a less increase in the AR. At 1 mM bulk concentration, a heavily charged particle can even produce a negative current change.

Conclusions

A comprehensive study using continuum models is conducted to investigate the effects of the access resistance on resistive-pulse caused by a translocating nanoparticle through a nanopore. For uncharged surfaces, we develop a correlation equation of α to estimate the effect of the access resistance at the blocked state. Using the approximate values of α, we are able to predict the current change caused by the translocation of a nanoparticle through a nanopore under various operating conditions. Moreover, we establish a cubic relation between the relative particle size and the current change in nanopores ranging from high aspect-ratio to low aspect-ratio. Based on the cubic relation, a simple but effective method is proposed to estimate the resistive-pulse amplitude. For charged surfaces, the ratio of access resistance to pore resistance will increase if the nanopore or the particle surfaces are charged more, suggesting that the role of access resistance becomes more important. We also find that the shape of the position-dependent resistive-pulse might be distorted significantly at low bulk concentration due to concentration polarization. This study provides a deep insight into the mechanism of access resistance in nanopore systems and will be helpful in interpreting experimental results for nanoparticle translocation.

Acknowledgements

This work was financially supported by MOST(2011CB707604), NSFC (11272321, 11102214), and MOST(2011CB707601). We thank Drs Xu Zheng and Zhanhua Silber-Li at LNM for the helpful discussion.

Notes and references

1 W. H. Coulter, *US Pat.*, 2656508, 1953.
2 G. Brecher, M. Schneiderman and G. Z. Williams, *Am. J. Clin. Pathol.*, 1956, **26**, 1439–1449.

3 H. E. Kubitschek, *Nature*, 1958, **182**, 234–235.
4 J. Hirsch and E. Gallian, *J. Lipid Res.*, 1968, **9**, 110–119.
5 X. D. Wu, Y. J. Kang, Y. N. Wang, D. Y. Xu, D. Y. Li and D. Q. Li, *Electrophoresis*, 2008, **29**, 2754–2759.
6 J. S. Sun, Y. J. Kang, E. M. Boczko and X. Y. Jiang, *Electroanalysis*, 2013, **25**, 1023–1028.
7 S. Garaj, W. Hubbard, A. Reina, J. Kong, D. Branton and J. A. Golovchenko, *Nature*, 2010, **467**, 190–193.
8 M. Wanunu, T. Dadosh, V. Ray, J. M. Jin, L. McReynolds and M. Drndic, *Nat. Nanotechnol.*, 2010, **5**, 807–814.
9 B. Cressiot, A. Oukhaled, G. Patriarche, M. Pastoriza-Gallego, J.-M. Betton, L. Auvray, M. Muthukumar, L. Bacri and J. Pelta, *ACS Nano*, 2012, **6**, 6236–6243.
10 N. Arjmandi, W. Van Roy, L. Lagae and G. Borghs, *Anal. Chem.*, 2012, **84**, 8490–8496.
11 A. Ramachandran, Q. Guo, S. M. Iqbal and Y. Liu, *J. Phys. Chem. B*, 2011, **115**, 6138–6148.
12 R. R. Henriquez, T. Ito, L. Sun and R. M. Crooks, *Analyst*, 2004, **129**, 478.
13 B. M. Venkatesan and R. Bashir, *Nat. Nanotechnol.*, 2011, **6**, 615–624.
14 A. Oukhaled, L. Bacri, M. Pastoriza-Gallego, J. M. Betton and J. Pelta, *ACS Chem. Biol.*, 2012, **7**, 1935–1949.
15 M. Wanunu, *Phys. Life Rev.*, 2012, **9**, 125–158.
16 E. C. Gregg and K. D. Steidley, *Biophys. J.*, 1965, **5**, 393–405.
17 R. W. Deblois and C. P. Bean, *Rev. Sci. Instrum.*, 1970, **41**, 909–915.
18 R. W. DeBlois, C. P. Bean and R. K. A. Wesley, *J. Colloid Interface Sci.*, 1977, **61**, 323–335.
19 O. A. Saleh, *A novel resistive pulse sensor for biological measurements, (Ph.D thesis)*, Princeton University, 2003.
20 Z. P. Qin, J. A. Zhe and G. X. Wang, *Meas. Sci. Technol.*, 2011, **22**, 045804.
21 J. E. Hall, *J. Gen. Physiol.*, 1975, **66**, 531–532.
22 M. Davenport, K. Healy, M. Pevarnik, N. Teslich, S. Cabrini, A. P. Morrison, Z. S. Siwy and S. E. Létant, *ACS Nano*, 2012, **6**, 8366–8380.
23 I. Vodyanoy and S. M. Bezrukov, *Biophys. J.*, 1992, **62**, 10–11.
24 S. M. Bezrukov and I. Vodyanoy, *Biophys. J.*, 1993, **64**, 16–25.
25 V. Levadny, V. M. Aguilella and M. Belaya, *Biochim. Biophys. Acta, Biomembr.*, 1998, **1368**, 338–342.
26 M. Aguilella-Arzo, V. M. Aguilella and R. Eisenberg, *Eur. Biophys. J.*, 2005, **34**, 314–322.
27 D. G. Luchinsky, R. Tindjong, I. Kaufman, P. V. E. McClintock and R. S. Eisenberg, *Phys. Rev. E: Stat., Nonlinear, Soft Matter Phys.*, 2009, **80**, 021925.
28 C. Hyun, R. Rollings and J. Li, *small*, 2012, **8**, 385–392.
29 F. Farahpour, A. Maleknejad, F. Varnik and M. R. Ejtehadi, *Soft Matter*, 2013, **9**, 2750–2759.
30 S. W. Kowalczyk, A. Y. Grosberg, Y. Rabin and C. Dekker, *Nanotechnology*, 2011, **22**, 315101.
31 S. W. Kowalczyk and C. Dekker, *Nano Lett.*, 2012, **12**, 4159–4163.
32 Y. Yan, Q. Sheng, C. M. Wang, J. M. Xue and H. C. Chang, *J. Phys. Chem. C*, 2013, **117**, 8050–8061.
33 C. A. Merchant, K. Healy, M. Wanunu, V. Ray, N. Peterman, J. Bartel, M. D. Fischbein, K. Venta, Z. Luo, A. T. Johnson and M. Drndic, *Nano Lett.*, 2010, **10**, 2915–2921.
34 G. F. Schneider, S. W. Kowalczyk, V. E. Calado, G. Pandraud, H. W. Zandbergen, L. M. K. Vandersypen and C. Dekker, *Nano Lett.*, 2010, **10**, 3163–3167.
35 A. S. Prabhu, T. Z. N. Jubery, K. J. Freedman, R. Mulero, P. Dutta and M. J. Kim, *J. Phys.: Condens. Matter*, 2010, **22**, 454107.
36 L. Bacri, A. G. Oukhaled, B. Schiedt, G. Patriarche, E. Bourhis, J. Gierak, J. Pelta and L. Auvray, *J. Phys. Chem. B*, 2011, **115**, 2890–2898.
37 M. Tsutsui, S. Hongo, Y. H. He, M. Taniguchi, N. Gemma and T. Kawai, *ACS Nano*, 2012, **6**, 3499–3505.
38 M. Tsutsui, Y. Maeda, Y. H. He, S. Hongo, S. Ryuzaki, S. Kawano, T. Kawai and M. Taniguchi, *Appl. Phys. Lett.*, 2013, **103**, 013108.
39 C. Lee, L. Joly, A. Siria, A.-L. Biance, R. Fulcrand and L. Bocquet, *Nano Lett.*, 2012, **12**, 4037–4044.
40 H. Daiguji, *Chem. Soc. Rev.*, 2010, **39**, 901–911.
41 L. H. Yeh, M. K. Zhang, N. Hu, S. W. Joo, S. Z. Qian and J. P. Hsu, *Nanoscale*, 2012, **4**, 5169–5177.
42 L. H. Yeh, M. K. Zhang, S. Z. Qian and J. P. Hsu, *Nanoscale*, 2012, **4**, 2685–2693.
43 X. Xuan and D. Li, *Electrophoresis*, 2007, **28**, 627–634.
44 M. Mao, S. Ghosal and G. Hu, *Nanotechnology*, 2013, **24**, 245202.
45 M. S. Kilic, M. Z. Bazant and A. Ajdari, *Phys. Rev. E: Stat., Nonlinear, Soft Matter Phys.*, 2007, **75**, 021503.
46 H. Wang, A. Thiele and L. Pilon, *J. Phys. Chem. C*, 2013, **117**, 18286–18297.
47 S. Qian, A. Wang and J. K. Afonien, *J. Colloid Interface Sci.*, 2006, **303**, 579–592.
48 T. Z. Jubery, A. S. Prabhu, M. J. Kim and P. Dutta, *Electrophoresis*, 2012, **33**, 325–333.
49 J. Newman and K. E. Thomas-Alyea, *Electrochemical systems*, John Wiley & Sons, Hoboken, New Jersey, 2004.
50 H. Chang, F. Kosari, G. Andreadakis, M. A. Alam, G. Vasmatzis and R. Bashir, *Nano Lett.*, 2004, **4**, 1551–1556.
51 R. Schoch, J. Han and P. Renaud, *Rev. Mod. Phys.*, 2008, **80**, 839–883.

